Impaired B cell function during viral infections due to PTEN-mediated inhibition of the PI3K pathway

Andrew Getahun,[1,3] Scott M. Wemlinger,[1,3] Pratyaydipta Rudra,[4] Mario L. Santiago,[2] Linda F. van Dyk,[1,3] and John C. Cambier[1,3]

[1]Department of Immunology and Microbiology and [2]Division of Infectious Disease, University of Colorado School of Medicine, Aurora, CO 80045
[3]Department of Biomedical Research, National Jewish Health, Denver, CO 80206
[4]Department of Biostatistics and Informatics, University of Colorado School of Public Health, Aurora, CO 80045

Transient suppression of B cell function often accompanies acute viral infection. However, the molecular signaling circuitry that enforces this hyporesponsiveness is undefined. In this study, experiments identify up-regulation of the inositol phosphatase PTEN (phosphatase and tensin homolog) as primarily responsible for defects in B lymphocyte migration and antibody responses that accompany acute viral infection. B cells from mice acutely infected with gammaherpesvirus 68 are defective in BCR- and CXCR4-mediated activation of the PI3K pathway, and this, we show, is associated with increased PTEN expression. This viral infection–induced PTEN overexpression appears responsible for the suppression of antibody responses observed in infected mice because PTEN deficiency or expression of a constitutively active PI3K rescued function of B cells in infected mice. Conversely, induced overexpression of PTEN in B cells in uninfected mice led to suppression of antibody responses. Finally, we demonstrate that PTEN up-regulation is a common mechanism by which infection induces suppression of antibody responses. Collectively, these findings identify a novel role for PTEN during infection and identify regulation of the PI3K pathway, a mechanism previously shown to silence autoreactive B cells, as a key physiological target to control antibody responses.

INTRODUCTION

Host–pathogen interactions can initiate dynamic processes that alter the ability of the immune system to respond to immunogenic challenge. Depending on the pathogen and the timing of immunization or secondary infection, immune responses can be enhanced or suppressed. Whereas enhancement of immune responses can be advantageous to the host (Barton et al., 2007; Furman et al., 2015), suppression can have dire consequences (Elsner et al., 2015; Matar et al., 2015).

The effect of systemic infection on immune cell behavior has been an area of extensive investigation. However, relatively little is known regarding effects on B cell function. Although it has been recognized for >40 yr that the ability of infected hosts to mount antibody responses to subsequent challenges is impaired during and after certain acute infections (Notkins et al., 1970; Getahun et al., 2012; and the references therein), the molecular targets of suppression are unclear.

Why infections suppress immune responses is unclear. It could be an immune evasion strategy used by the pathogen or a feedback mechanism of the immune system. The observed delay in antiviral responses during infections with viruses that cause B cell suppression (Stevenson and Doherty, 1998) would suggest the former. In support for the latter possibility is the observation that infection often leads to polyclonal B cell activation during the acute phase of infection. Suppression of the ability to mount antibody responses could be a host mechanism to prevent bystander activation, which could lead to unwanted antibody response to self-antigens.

Previously, we examined the effects of systemic mouse gammaherpes virus 68 (γHV68) infection on anergic self-reactive B cells and naive B cells and found that, although both populations are polyclonally activated and produce elevated basal levels of antibody, including autoreactive antibodies, they are suppressed in their ability to mount antibody responses upon antigen challenge (Getahun et al., 2012). Both antigen-specific IgM and IgG responses, including germinal center formation, are suppressed in γHV68-infected mice (Getahun et al., 2012; Matar et al., 2015). We further found that B cells isolated from infected mice display dampened calcium mobilization after B cell receptor (BCR) cross-linking, suggesting altered intracellular signaling. The effects of infection are not limited to cells harboring the virus, as signaling is modulated in all B cells. These results are most consistent with infection-induced production of soluble mediators that cause global B cell suppression.

Silencing of autoreactive B cells in the periphery is mediated by alterations in BCR signaling induced by chronic exposure to antigen (Cooke et al., 1994). Thus, autoreactive

Correspondence to John C. Cambier: john.cambier@ucdenver.edu

Abbreviations used: AFC, antibody-forming cell; BCR, B cell receptor; d.p.i., days postinfection; FV, Friend retrovirus; HEL, hen egg lysozyme; LDV, lactate-dehydrogenase–elevating virus; MCMV, mouse CMV; MFI, mean fluorescence intensity; PI3K, phosphoinositide 3-kinase; PTEN, phosphatase and tensin homolog; SRBC, sheep RBC; WCL, whole-cell lysate; YFP, yellow fluorescent protein.

The Rockefeller University Press $30.00
J. Exp. Med. 2017 Vol. 214 No. 4 931–941
https://doi.org/10.1084/jem.20160972

B cells whose antigen receptors have intermediate avidity for self-antigens escape central tolerance mechanisms operative in the bone marrow and persist in the periphery in a state of unresponsiveness called anergy. Multiple antigen receptor-coupled signaling pathways that promote cell activation are inhibited in anergic B cells because of increased activity in inhibitory signaling by phosphatases such as SH2-containing tyrosine phosphatase 1 (SHP-1), SH2-containing inositol 5–phosphatase 1 (SHIP-1), and phosphatase and tensin homolog (PTEN; Getahun et al., 2016). The latter two are inositol phosphatases that dephosphorylate PtdIns(3,4,5)P3, thereby opposing the effect of phosphoinositide 3-kinase (PI3K) activation, which is required for BCR-mediated cell activation. Negative regulation of the PI3K pathway is required to prevent autoreactive B cells from making antibody responses (Browne et al., 2009; Akerlund et al., 2015; Getahun et al., 2016).

In this study, we examined the ability of antigen receptors on B cells from γHV68-infected mice to transduce signals after stimulation. We found that these B cells are inhibited in their ability to activate the PI3K pathway after BCR and CXCR4 stimulation and determined that this is because of increased expression of PTEN. This viral infection-induced PTEN overexpression contributes to the observed suppression of antibody responses in infected mice, as PTEN deficiency or expression of a constitutively active PI3K rescued the ability of B cells to mount antibody responses in infected mice. We further provide evidence that this mechanism is operative during infection by additional viruses that suppress antibody responses. Finally, we show that B cell–targeted overexpression of PTEN without other confounding effects of infection or self-antigen exposure is sufficient to suppress antibody responses.

RESULTS AND DISCUSSION

B cells from γHV68-infected mice have suppressed PI3K signaling

Previously, we demonstrated that B cells isolated from γHV68-infected animals have reduced ability to mobilize calcium in response to IgM cross-linking (Getahun et al., 2012). Assuming that this defect in BCR signaling is in part responsible for the observed reduced ability to mount antibody responses after acute infection, we analyzed activation of key upstream components in the signaling cascade triggered by BCR cross-linking. First, we extended our initial findings by testing the ability of B cells from acutely γHV68-infected mice to mobilize calcium after IgM and IgD cross-linking. Although both receptors were expressed on the cell surface at levels comparable with uninfected controls, B cells from γHV68-infected mice had reduced ability to mobilize calcium upon receptor cross-linking (Fig. 1 A). Analysis of global tyrosine phosphorylation after IgM cross-linking did not reveal gross defects or changes in phosphorylation relative to B cells from infected mice (Fig. 1 B). Similarly, phosphorylation of Syk, one of the earliest events that follow BCR stimulation, was comparable between B cells from infected and sham-infected animals (Fig. 1 C). Further downstream, activation of Erk was normal in B cells from infected mice, but phosphorylation of PLCγ2 and Akt was reduced (Fig. 1 D). Both of these events are dependent on the accumulation of plasma membrane PI(3,4,5)P3, which binds their pleckstrin homology domains, capturing the enzymes, thus improving access of activating kinases. PI(3,4,5)P3 is generated by PI3K, suggesting a defect in the PI3K pathway in infected mice. Interestingly, suppression of the PI3K pathway has previously been shown to be a major mechanism by which peripheral autoreactive B cells are functionally silenced (Browne et al., 2009; Akerlund et al., 2015; Getahun et al., 2016).

To determine whether this signaling defect is unique to signaling through the BCR, we examined CXCR4 signal transduction. CXCR4 is a chemokine receptor expressed on B cells that responds to its ligand, SDF-1 or CXCL12, by PI3K-dependent activation of migration (Brauweiler et al., 2007). First, we tested the ability of B cells from γHV68-infected and control mice to migrate to SDF-1 in a transwell migration assay. B cells from infected animals had a reduced ability to migrate in response to SDF-1 (Fig. 1, E and F). This was not caused by altered CXCR4 expression (Fig. 1 G) but, rather, appeared to be caused by decreased signaling through the PI3K pathway, as it was associated with decrease SDF-1–stimulated Akt phosphorylation (Fig. 1 H). These results support the notion that there is a global defect in PI3K signaling in B cells from infected mice. In addition, they suggest that defects in cell migration in infected mice (Benedict et al., 2006; Mueller et al., 2007) may not only be caused by expression of viral encoded chemokines (Martin et al., 2006), but also is, in part, a consequence of impaired signaling through the chemokine receptors.

PTEN expression is elevated in B cells from infected mice and is required for suppression of antibody responses

The PI3K pathway is regulated by the inositol phosphatases SHIP-1 and PTEN that dephosphorylate PI(3,4,5)P3, yielding PI(3,4)P2 and PI(4,5)P2, respectively. PI3K is activated after BCR stimulation via CD19 and B cell adaptor for PI3K (BCAP). To determine whether reduced PI3K pathway activity in B cells from infected animals is caused by decreased PI3K activation, we examined the integrity of CD19 phosphorylation induced by BCR cross-linking. B cells from γHV68-infected and uninfected mice had comparable levels of CD19 tyrosine phosphorylation (Fig. 2 A), suggesting that activation of PI3K is normal. Next, we examined the activity of inositol phosphatases in B cells from γHV68-infected mice. B cells from control and γHV68-infected animals had comparable basal SHIP-1 and docking protein 1 (Dok; a SHIP-1 adaptor) phosphorylation (Fig. 2 B), suggesting similar SHIP-1 activity. In contrast, B cell expression of PTEN was elevated about twofold in γHV68-infected mice (Fig. 2 C). Elevated PTEN has been shown previously to limit the responsiveness of anergic B cells from soluble hen egg lysozyme (HEL; ML5) × HEL–reactive immunoglobulin (MD4)

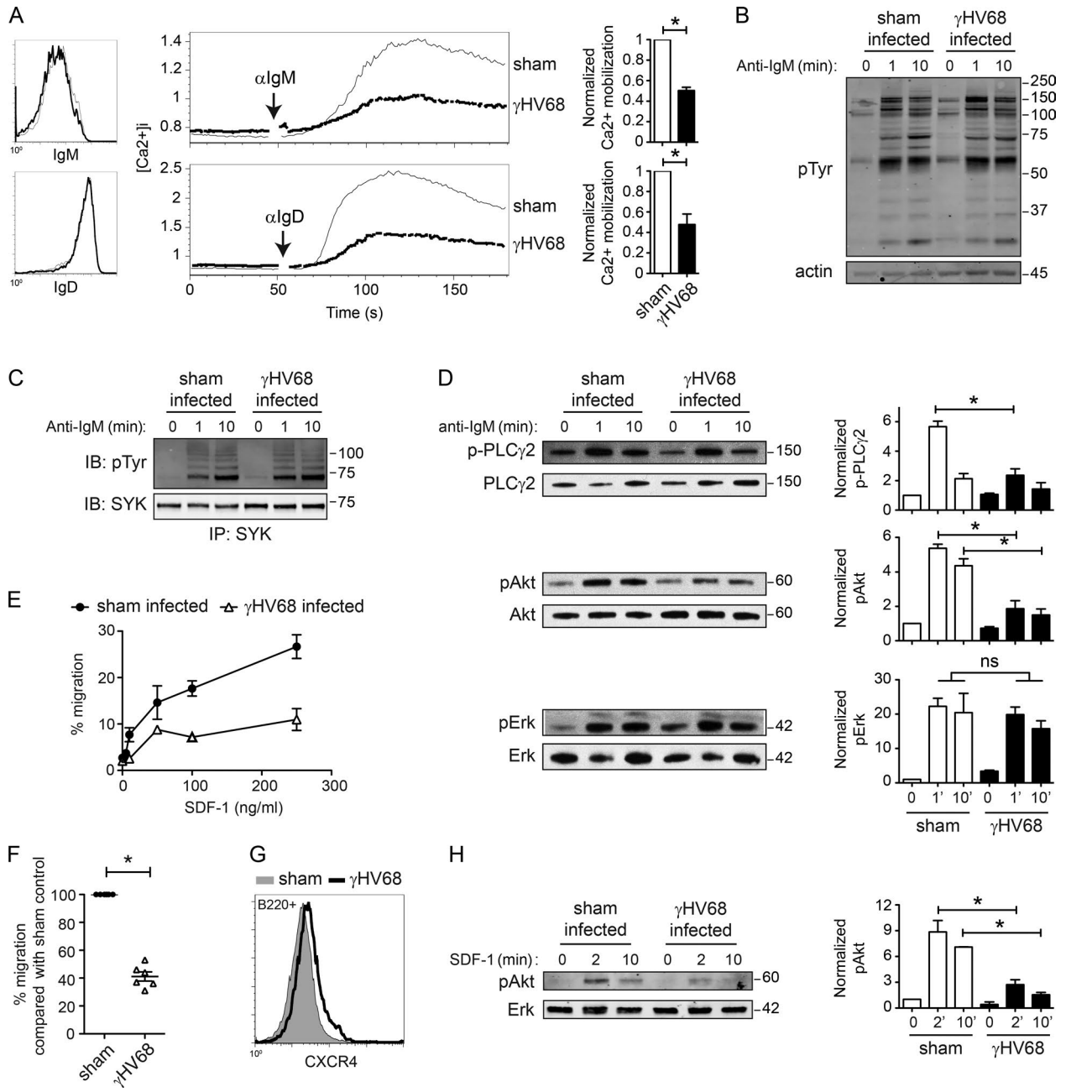

Figure 1. **B cells from γHV68-infected mice are suppressed in PI3K pathway signaling.** (A–H) Signaling characteristics of B cells from γHV68-infected mice (8 d.p.i.) or sham-infected mice. (A) Surface IgM and IgD expression (left), intracellular calcium mobilization after stimulation with 2.5 µg anti-IgM/ml or 0.2 µg anti-IgD/ml (n = 8; representative plots are shown; middle), and quantification of calcium responses normalized to the sham-infected response (right). (B) Whole-cell tyrosine phosphorylation after stimulation with 10 µg $F(Ab')_2$ anti-IgM/ml. n = 8. Representative blots are shown. (C) Syk phosphorylation after stimulation with 10 µg $F(Ab')_2$ anti-IgM/ml. n = 6. Representative blots are shown. IB, immunoblot; IP, immunoprecipitation. (D) PLCγ2, Akt, and Erk phosphorylation after stimulation with 10 µg $F(Ab')_2$ anti-IgM/ml (n = 6; representative blots are shown; left) and quantifications of phosphorylation normalized to unstimulated sham control (right). (E) Migration of B cells in response to increasing concentration of SDF-1. n = 2/experiment. (F) Relative migration of B cells to 100 ng SDF-1/ml compared with sham control B cells. Means are plotted of three independent experiments. n = 6. (G) CXCR4 surface expression on B cells ($B220^+$) from infected (thick line) or sham infected (shaded) mice. n = 4. Representative plots are shown. (H) Akt phosphorylation after stimulation with 100 ng SDF-1/ml (n = 4; a representative blot is shown; left) and quantification of phosphorylation normalized to unstimulated sham control (right). Data shown are representative of at least two replicate experiments. Error bars represent mean ± SEM. Both-tailed unpaired Student's t test (D and H) or both-tailed one-sample Student's t test (A and F) was used. ns, $P > 0.05$; *, $P < 0.05$. In immunoblots, mass is shown in kilodaltons.

transgenic mice (Browne et al., 2009). To determine whether PTEN is required for γHV68 infection–induced B cell unresponsiveness, we tested whether *PTEN*-deficient B cells are insensitive to infection-induced B cell suppression. To address this, we used an adoptive transfer approach combined with inducible deletion of *PTEN* in B cells (hCD20-Cre^{TAM} × ROSA26 STOPflox YFP × *PTEN*$^{fl/fl}$ × MD4) with a known specificity for HEL (Fig. 2 E). A model allowing inducible deletion of *PTEN* in the periphery was used to avoid the confounding effects of loss of PTEN on B cell development. The donor mice also contained a yellow fluorescent protein (YFP) reporter as an indicator of cre activity. Control MD4 mice expressed inducible cre and a YFP reporter but unaltered *PTEN* genes. Thus, although the B cells express YFP after tamoxifen treatment, they are *PTEN* sufficient. 6 d before adoptive transfer, cre activity was induced by tamoxifen treatment. On the day of adoptive transfer, YFP$^+$ B cells were isolated using FACS and adoptively transferred into mice that had been infected with γHV68 or sham infected 6 d earlier. We confirmed by Western blotting that sorted YFP$^+$ B cells were PTEN deficient at this time point (not depicted). 24 h later, mice were immunized with HEL–sheep RBCs (HEL-SRBCs), and 5 d later, the MD4-derived anti-HEL response was determined by ELISPOT. Between 24 and 36 h after adoptive transfer, *PTEN*-sufficient MD4 B cell up-regulate PTEN to comparable levels as host B cells in infected mice (Fig. 2 D). Host B cells had a 1.46 ± 0.12–fold increase in PTEN mean fluorescence intensity (MFI), whereas transferred MD4 B cells had a 1.40 ± 0.12–fold increase in PTEN MFI (infected vs. sham; 36 h after transfer; $n = 7$; $P > 0.05$; no statistical difference in fold-increase; unpaired Student's *t* test). As demonstrated previously (Getahun et al., 2012), *PTEN*-sufficient B cells adoptively transferred into infected mice acquired the suppressed phenotype and did not make a detectable antibody response (Fig. 2 F). In contrast, *PTEN*-deficient B cells transferred into infected mice made comparable antibody responses to those transferred into sham-infected mice (Fig. 2 F). This suggests that elevated PTEN levels in B cells of infected mice suppress the ability of these B cells to mount antibody responses. PTEN has several biological functions beyond negative regulation of the PI3K pathway (for review, see Song et al., 2012). To determine whether reduction of PI(3,4,5)P3 levels by PTEN is responsible for the observed inhibition, we introduced an inducible, constitutively active PI3K into our experimental system, reasoning that its activity should counteract the increased inositol phosphatase activity. A similar experimental approach was used as described for *PTEN* deletion. The immune response of B cells from infected mice was rescued by constitutively active PI3K (Fig. 2 G). These results further strengthen the hypothesis that inhibition of the PI3K pathway is responsible for reduced antibody responses of B cells in γHV68-infected mice.

Suppression of antibody responses after acute viral infection is not unique to γHV68 infection. To determine whether up-regulation of PTEN is associated with suppression of humoral immune responses during other viral infections, we assayed PTEN levels in B cells from mice infected with mouse CMV (MCMV) or Friend retrovirus (FV). Infection by either virus reportedly causes polyclonal B cell activation and is associated with a period of immune suppression (Howard and Najarian, 1974; Ceglowski et al., 1975). In our experiments, we used lactate-dehydrogenase–elevating virus (LDV)–free FV because coinfection causes additional suppression of immune responses by a mechanism that is still unclear but appears to involve polyclonal B cell activation by LDV (Marques et al., 2008). First, we confirmed the previously reported kinetics of onset of suppression (immunization 3 d postinfection [d.p.i.] for LDV-free FV infection and immunization 6 d.p.i. for MCMV infection; Fig. 2 H, top). At these time points, B cells isolated from LDV-free FV and MCMV-infected mice expressed elevated PTEN levels (Fig. 2 H, bottom), suggesting a role for PTEN in the observed suppression. Not all viral infections are associated with periods of reduced immune competence. Although there is some conflicting data, most studies suggest that LDV infection does not affect antibody responses and, in some situations, may even enhance antibody responses (Michaelides and Simms, 1977; Isakov et al., 1982). In an effort to further probe the relationship between up-regulation of PTEN and suppressed immune competence, we determined the effect of LDV infection on PTEN levels and the ability to mount antibody responses. We observed no significant elevation in PTEN, nor were antibody responses suppressed after infection (Fig. 2, I and K). There was transient up-regulation of B cell activation markers CD86 and CD69 1 d after infection (Fig. 2 J). These results indicate that PTEN up-regulation is not a general consequence of viral infection and support the notion that PTEN up-regulation is required for suppression after infection by certain viral pathogens. The mechanism by which PTEN up-regulation is induced is still unknown and currently under investigation.

Increased B cell expression of PTEN is sufficient to suppress antibody responses

Infection causes many acute changes in the immune system including alterations in lymphoid architecture (Benedict et al., 2006; Mueller et al., 2007) and production of cytokines that alter immune responses. To test the effect of increased PTEN expression on B cell responses without the confounding effects of infection, we generated a new mouse model (Fig. 3 A) that allows inducible overexpression of PTEN uniquely in the B cell compartment. Floxed-stop *PTEN* followed by a 2A peptide sequence and YFP was knocked into the *Rosa26* locus. In this system, the 2A peptide sequence, separating the fused PTEN and YFP, is cleaved in vivo yielding equimolar quantities of each. This line was crossed with the hCD20 Cre^{TAM}-transgenic mouse, and after tamoxifen activation of Cre^{TAM}, many B cells expressed YFP and increased PTEN (Fig. 3 B). The PTEN elevation was comparable with that observed in B cells from γHV68-infected mice

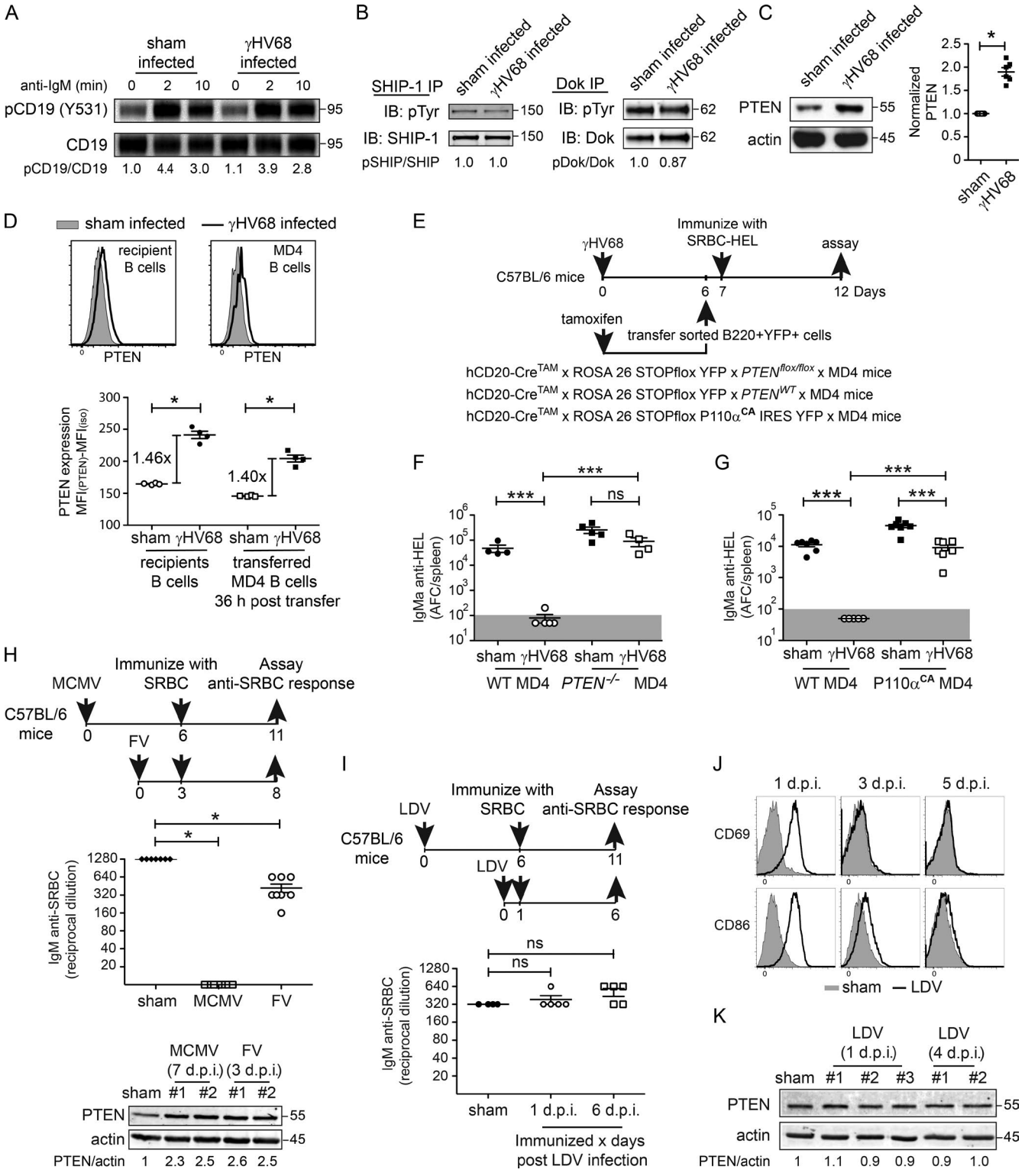

Figure 2. **B cells from infected mice express elevated PTEN causing suppression of antibody responses.** (A–D) Signaling characteristics of B cells from sham- or γHV68-infected mice (8 d.p.i.). (A) CD19 phosphorylation after stimulation with 10 µg $F(Ab')_2$ anti-IgM/ml. $n = 8$. A representative blot is shown. (B) Basal SHIP-1 phosphorylation (left) and basal Dok phosphorylation (right). $n = 6$. Representative blots are shown. IB, immunoblot; IP, immunoprecipitation. (C) Basal PTEN expression ($n = 6$; a representative blot is shown; left) and quantification of PTEN levels normalized to sham control of six independent experiments (right). (D) PTEN expression in MD4 B cells 36 h after transfer into mice infected with γHV68 6 d earlier or sham-infected mice, compared with PTEN expression in B cells from the recipient/host mice. $n = 3$–4/group/experiment. iso, isotype. (E) Schematic representation of the

and anergic MD4 × ML5 B cells (Fig. 3 C). MD4 × ML5 B cells are autoreactive and have previously been shown to be silenced in part by PTEN up-regulation and subsequent PI3K pathway suppression (Browne et al., 2009).

We used the inducible PTEN overexpression model described above to determine the effect of acute PTEN overexpression on BCR signaling. Whereas surface IgM and IgD expression are unchanged, PTEN overexpressing B cells exhibited dampened calcium mobilization after antigen receptor cross-linking (Fig. 3 D), as observed in B cells of γHV68-infected mice (Fig. 1 A). Similarly, both basal Akt phosphorylation and stimulated Akt phosphorylation were reduced in PTEN-overexpressing B cells, whereas Syk phosphorylation was unchanged (Fig. 3 E). These results are consistent with suppression in the PI3K pathway, whereas upstream signaling is spared. In contrast, MD4 × ML5 B cells exhibited additional signaling defects in calcium mobilization (Fig. 3 D) and Syk phosphorylation (Fig. 3 E), potentially attributable to both decreased IgM expression (Kirchenbaum et al., 2014) and additional inhibitory signaling by SHIP-1 (Akerlund et al., 2015) and SHP-1 (Getahun et al., 2016). Finally, we determined the effect of PTEN overexpression on the ability of B cells to mount an antibody response. Using a similar adoptive transfer approach (Fig. 3 F) as in Fig. 2, we found that B cells with elevated PTEN expression had a significantly reduced ability to mount antibody responses (Fig. 3 G). A mean of four independent experiments revealed a reduction in antibody-forming cell numbers of ∼70% (Fig. 3 H). Combined, these results demonstrate that PTEN overexpression is sufficient for the signaling defects observed in B cells from virus-infected mice and contributes to their reduced ability to mount antibody responses. The degree of suppression observed differs among different infections (Fig. 2 H), and although the reduction in antibody responses during FV infection (∼70%) could be explained by suppressive effects of PTEN overexpression alone (Fig. 3 H), the >99% suppression observed during γHV68 and MCMV infections suggests that additional factors play a role in suppression. The fact that PTEN deletion in B cells rescues the suppression phenotype (Fig. 2 D), whereas overexpression of PTEN in B cells to comparable levels as B cells from infected mice only accounts for up to 70% of the suppression observed (Fig. 3 H), suggests that PTEN may be involved in regulating other signals that contribute to the suppression phenotype as well.

The data described in this paper define a previously unidentified mechanism of virus infection–induced immune suppression. These findings and previous work on regulation of B cell tolerance (Browne et al., 2009; Akerlund et al., 2015; Getahun et al., 2016) demonstrate that the PI3K pathway is a target for physiological regulation of B cell function. Interestingly, T cell function is suppressed during measles infection because of suppression of the PI3K pathway by a SHIP-1 splice variant (Avota et al., 2006), suggesting that this pathway may be a common target in infection-induced immune suppression. Because PTEN has recently been implicated to play a role in IRF3 activation and antiviral immunity (Li et al., 2016), it is possible that the observed suppression is a side effect of the induction of an antiviral response. Regardless, given the consequences of suppression of antibody response on the ability to control secondary infections (Elsner et al., 2015; Matar et al., 2015) and potentially the efficacy of vaccination (Holder et al., 2010), this is an issue that deserves further investigation.

MATERIALS AND METHODS

Mice

Except where otherwise indicated, 6–16-wk-old mice were used in all experiments. Both male and female mice were used. Experiments were sex matched, and both sexes gave identical results. C57BL/6 mice were used in all experiments involving infection. C57BL/6, MD4, and MD4 × ML5 mice (Goodnow et al., 1988) were used in PTEN overexpression and signaling experiments. To generate mice in which *PTEN* deletion can be induced in MD4 B cells, hCD20-CreTAM animals (gift from M. Shlomchik, University of Pittsburgh, Pittsburgh, PA; Khalil et al., 2012) were intercrossed with mice carrying the rosa26-STOPflox-YFP allele (Srinivas et al., 2001), generating mice in which YFP is expressed in B cells upon Cre activation. These mice were crossed with MD4 B cell antigen receptor–transgenic mice to generate hCD20-CreTAM × rosa26-STOPflox-YFP × MD4 mice. B cells from these mice will be referred to as WT MD4. These mice were crossed to $PTEN^{flox/flox}$ mice (gift from R. Rickert, Sanford Burnham Prebys Medical Discovery Institute, La Jolla, CA; Anzelon et al., 2003) to generate mice in which PTEN deletion can be induced in MD4 B cells. To generate mice in which MD4 B cells can be induced to express a constitutively active PI3K pathway, hCD20-CreTAM ×

experimental protocol. IRES, internal ribosome entry site. (F) Day-5 IgM^a anti-HEL antibody-forming cell (AFC) response of *PTEN*-sufficient and -deficient MD4 B cells in sham- and γHV68-infected mice. n = 4–5/group/experiment. The gray area delineates the limit of detection (100 spots/spleen). (G) Day-5 IgM^a anti-HEL AFC response of MD4 B cells expressing a constitutively active PI3K or control MD4 B cells in sham- or γHV68-infected mice. n = 5–7/group/experiment. The gray area delineates the limit of detection (100 spots/spleen). (H, top) IgM anti-SRBC response of mice infected with MCMV (immunized at 6 d.p.i.) or FV (immunized at 3 d.p.i.). n = 6–7/group/experiment. (Bottom) PTEN expression in B cells from MCMV-infected (7 d.p.i.), FV-infected (3 d.p.i.), and sham-infected mice. n = 6. Representative blots are shown. (I) IgM anti-SRBC response of mice infected with LDV (immunized at 1 or 6 d.p.i.). n = 4–5/group/experiment. (J) Expression of activation markers on splenic B cells (gated on B220) from mice infected with LDV at the indicated times after infection. n = 9. Representative plots are shown. (K) PTEN expression in B cells from several LDV-infected mice (1 and 4 d.p.i.). n = 6. Representative blots are shown. Data shown are representative of at least two replicate experiments. Error bars represent mean ± SEM. Both-tailed unpaired Student's t test (D, F–H, and I) or both-tailed one-sample Student's t test (C) was used. ns, $P > 0.05$; *, $P < 0.05$; ***, $P < 0.001$. In immunoblots, mass is shown in kilodaltons.

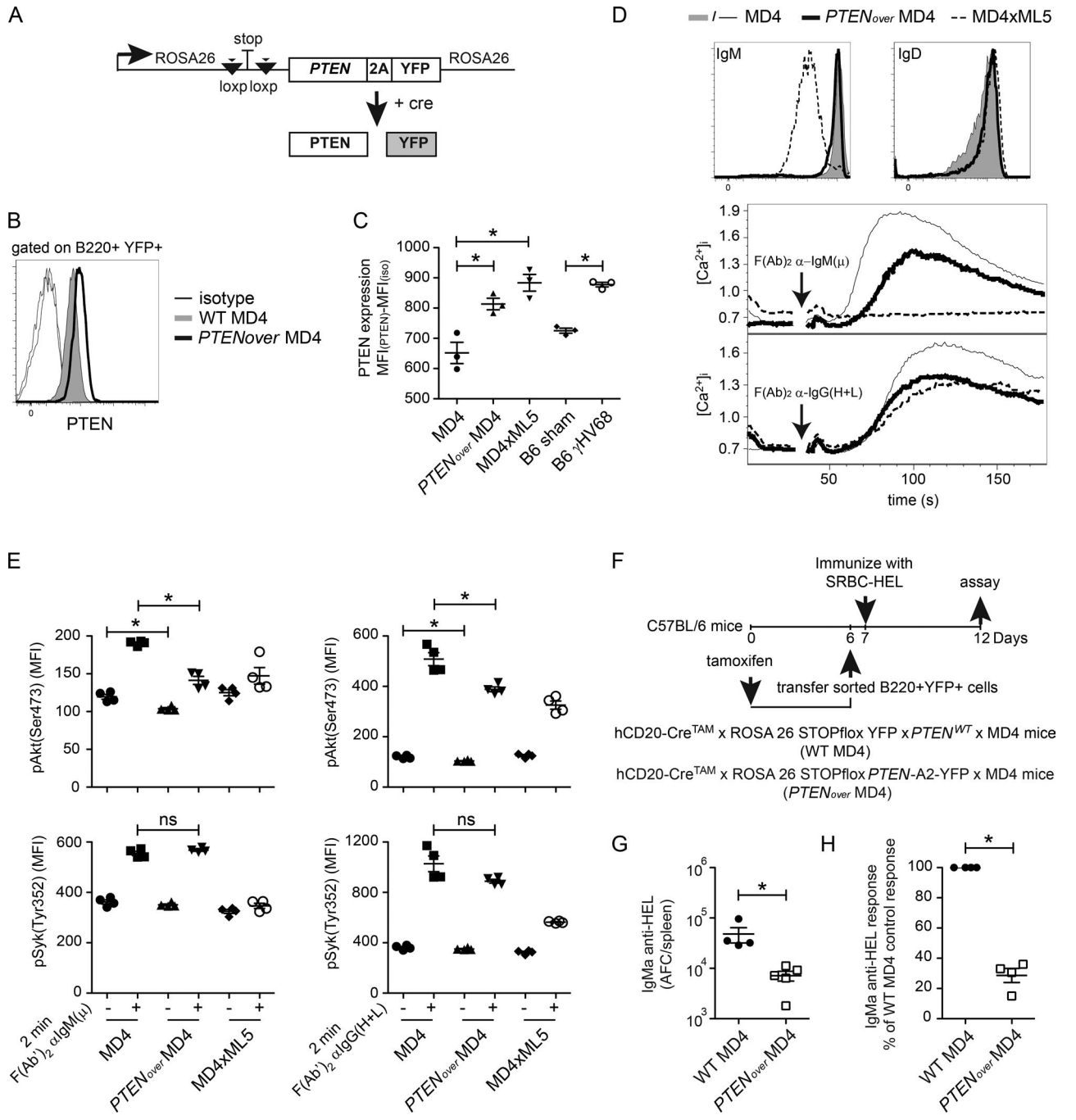

Figure 3. **B cell–targeted PTEN overexpression suppresses antibody responses.** (A) Schematic representation of the inducible PTEN overexpression construct used to create the hCD20-CreTAM × ROSA26 STOPflox *PTEN*-2A-YFP knock-in mice. (B) PTEN expression measured by intracellular flow cytometry in YFP$^+$ B220$^+$ cells of the mice described in Fig. 3 F 6 d after tamoxifen treatment. $n = 8$. A representative plot is shown. PTENover, PTEN overexpression. (C) PTEN expression (PTEN MFI and isotype [iso] control MFI) by B cells from MD4, YFP$^+$ *PTEN*-2A-YFP knock-in. MD4 mice 6 d after tamoxifen, MD4 × ML5, C57BL/6 sham-infected, or C57BL/6 γHV68-infected (7 d.p.i.) are shown. $n = 3$/group/experiment. (D) Surface IgM and IgD expression (top) and intracellular calcium mobilization (bottom) after stimulation with 1.25 µg F(Ab')$_2$ anti-IgM/ml or 1.25 µg F(Ab)$_2$ anti-IgG (H+L)/ml of MD4, MD4 × ML5, and hCD20-CreTAM × ROSA26 STOPflox *PTEN*-2A-YFP × MD4 B cells (YFP$^+$; 6 d after tamoxifen; gated on B220$^+$ events). $n = 6$. Representative plots are shown. (E) Phosphoflow analysis (pAkt and pSyk) of MD4, MD4 × ML5, and hCD20-CreTAM × ROSA26 STOPflox *PTEN*-2A-YFP × MD4 (YFP$^+$; 6 d after tamoxifen) B cells (gated on B220$^+$) after stimulation with 5 µg F(Ab)$_2$ anti-IgM/ml or 5 µg F(Ab)$_2$ anti-IgG (H+L)/ml for 2 min. $n = 4$/group/experiment. (F) Schematic representation of the experimental protocol for G and H. (G) Day-5 IgM^a anti-HEL AFC response of PTEN overexpressing MD4 B cells or control MD4 B cells. $n = 4$–5/group/experiment. (H) Relative day-5 IgM^a anti-HEL AFC response (compared with mean response by WT MD4 B cells) of four independent experiments as described in F and G. Data shown are representative of at least two replicate experiments. Error bars represent mean ± SEM. Both-tailed unpaired Student's *t* test (C, E, and G) or both-tailed one-sample Student's *t* test (H) was used. ns, $P > 0.05$; *, $P < 0.05$.

MD4 mice were crossed with Rosa26-flox-STOP-P110α-^{CA}-YFP mice (gift from K. Rajewsky, Max Delbruck Center for Molecular Medicine, Berlin, Germany; Srinivasan et al., 2009). These mice have a cassette encoding a constitutively active form of P110α, the catalytic subunit of PI3K, followed by an internal ribosome entry site and GFP gene and preceded by a *loxP*-flanked STOP cassette, knocked into the *rosa26* locus. To generate mice in which MD4 B cells can be induced to overexpress PTEN, hCD20-CreTAM × MD4 mice were crossed with Rosa26-STOPflox-*PTEN*-2A-YFP mice (described below). Mice were housed and bred in the Biological Resource Center at National Jewish Health or at the University of Colorado Denver Anschutz Medical Center Vivarium, with the exception of C57BL/6 mice, which were purchased from Jackson ImmunoResearch Laboratories, Inc. All experiments with mice were performed in accordance with the regulations and with approval of National Jewish Health and the University of Colorado Denver Institutional Animal Care and Use Committee.

Construction of Rosa26-STOPflox-*PTEN*-2A-YFP mouse

Rosa26-STOPflox-*PTEN*-2A-YFP mice were generated by the Mouse Genetics Core Facility at National Jewish Health. In these mice, a construct was knocked into the *rosa26* locus containing a STOP-flox cassette preventing transcription of a single transcript of *PTEN* cDNA flanked by a 2A peptide followed by YFP cDNA. Upon exposure to Cre recombinase, the stop cassette will be deleted. The PTEN-2A-YFP protein undergoes cleavage because of the 2A peptide, generating separate PTEN and YFP proteins. In brief, the targeting construct was made in a pBSKS-DTA vector. The *rosa26* genomic regions were isolated from bacterial artificial chromosome (BAC) clone PR23-324O18, PTEN was amplified from a C57BL/6 cDNA library, the STOPflox cassette (containing a positive selection marker Neo flanked by loxP sequences) was cloned from pBigT (no. 21270; Addgene), and 2A peptide was synthesized in the primers used to amplify YFP. Linearized construct was electroporated into JM8.A3 cells, and cells were selected with G418 (positive selection) for targeted insertion of the construct. Selected clones were picked and frozen. Successfully targeted homologous recombinant clones were determined by screening by loss of *Rosa26* allele quantitative PCR followed by PCR using a primer pair nested in *rosa26* and YFP. Functionality of the construct in the ROSA26 locus was verified on homologous recombinant embryonic stem cell clones by expansion and electroporation of these clones with plasmid expressing Cre recombinase. Expression was under the control of the CMV promoter. 2 d after electroporation, these embryonic stem cell clones were analyzed by flow cytometry to assess the expression of YFP in the absence or presence of Cre recombinase. Two clones were selected and injected into C57BL/6J blastocysts and implanted in C57BL/6J females. Chimeric offspring were bred for germline transmission, and three germline-competent chimeras were identified. Two independent lines were crossed with inducible cre and MD4 mice as described above and used in experiments with identical results.

Viruses and infections

γHV68 clone WUMS (VR1465; ATCC) was passaged, grown, and titered as previously described (Virgin et al., 1997). Mice were infected with 10^6 PFU by i.p. injection in 0.5 ml IMDM or sham infected with IMDM alone. MCMV was passaged and grown, and the virus titer was determined as previously described (Brown et al., 2001). Mice were infected with 10^6 PFU by i.p. injection in 0.5 ml IMDM or sham infected with IMDM alone. FV, a complex composed of B-tropic F-MuLV and spleen focus-forming virus SFFV, was prepared and titered in BALB/c mice (Santiago et al., 2008) and lacks LDV (Robertson et al., 2008). Mice were infected with 10^4 spleen focus-forming units in 200 µl DMEM by i.v. injection. LDV (a gift from K. Hasenkrug, National Institutes of Health, Bethesda, MD; Robertson et al., 2008) was prepared in C57BL/6 mice. Mice were infected by i.v. injection with 200 µl of pooled serum, diluted 1:100 in IMDM, and collected from mice 20–22 h after infection with LDV.

Antigens and immunization

SRBCs were purchased from the Colorado Serum Company and stored in sterile Alsever's solution at 4°C. The cells were washed three times in PBS before use, and mice were injected i.p. with 200 µl of 1% SRBC suspension. For experiments with MD4 B cells, HEL was chemically coupled to SRBCs. 1 ml of packed SRBCs were resuspended in 15 ml PBS containing 5 mg/ml HEL (Sigma-Aldrich). To cross-link, 1 ml of 50 mg/ml 1-ethyl-3-(3-dimethylaminopropyl)carbodiimide hydrochloride (Sigma-Aldrich) in PBS was added, mixed, and incubated for 1 h at room temperature, with occasional mixing. Afterward, the cells were washed four times in PBS, and the conjugation of HEL to the SRBC cell surface was confirmed by flow cytometry after staining with Dylight 650–conjugated anti-HEL (clone D1.3).

Adoptive transfers and Cre induction

CreTAM activation was induced by tamoxifen administration in MD4 donor mice leading to the expression or deletion of proteins of interest. Tamoxifen (T-5648; 20 mg/ml final concentration; Sigma-Aldrich) was dissolved in corn oil (Sigma-Aldrich) containing 10% ethanol (Decon Laboratories). 100 µl (2 mg) was injected i.p. on two consecutive days. 6 d after the first tamoxifen injection, spleens were harvested for subsequent experiments. At this time, deletion or expression of the proteins of interest was confirmed by immunoblotting or intracellular immunofluorescence. MD4 donor cells were stained with anti-B220–APC, and YFP^+ $B220^+$ events were sorted on a MoFlo XDP (Beckman Coulter) or an ICyt Synergy (Sony) cell sorter. 5×10^4–2×10^5 YFP^+ $B220^+$ cells were adoptively transferred by i.v. injection in 200 µl PBS at the indicated times after infection or in sham-infected mice or uninfected mice. 24 h after transfer, the mice were im-

munized by i.p. injection with 200 µl of 1% SRBC-HEL. 5 d later, serum and splenocytes were harvested and analyzed for anti-HEL responses.

Flow cytometry

Cells were resuspended in PBS containing 1% BSA and 0.05% sodium azide and incubated with an optimal amount of directly fluorochrome-labeled antibodies. Antibodies directed against the following molecules were used: B220 (RA3-6B2; BD), CD86 (GL1; BD), CD69 (H1.2F3; BD), IgM (b76), IgD (11-26; SouthernBiotech), and CXCR4 (2B11; BD). B-7-6 was produced in our own laboratory and was directly conjugated to DyLight (Thermo Fisher Scientific) fluorochromes, according to the manufacturer's protocol. For detection of intracellular PTEN, splenocytes were first stained with B220-BV510, fixed and permeabilized with Cytofix/Cytoperm (BD), and stained with anti-PTEN–Alexa Fluor 647 (clone A2B1; BD) or IgG1κ–Alexa Fluor 647 isotype control (MOPC-21; BD). In some cases, cells were also stained with anti-GFP (goat anti-GFP; Rockland) conjugated to DyLight 488 (Thermo Fisher Scientific; according to the manufacturer's protocol) to amplify YFP signal.

For analysis of protein phosphorylation by flow cytometry, splenocytes were resuspended in serum-free IMDM at a concentration of 10^7 cells/ml and incubated at 37°C for 30–60 min before stimulation with 5 µg/ml $F(Ab')_2$ goat anti–mouse IgM (anti-µ; Jackson ImmunoResearch Laboratories, Inc.) or 5 µg/ml $F(Ab')_2$ rabbit anti–mouse IgG (H+L; Invitrogen) for the indicated times. Signaling was stopped by adding formaldehyde at a final concentration of 2% and incubated at 37°C for 10 min. The cells were spun down and resuspended in 100% MeOH (directly from −80°C) and incubated on ice for 30 min. At this point, the cells were either processed further or stored at −20°C for later analysis. After permeabilization, the cells were washed twice in PBS containing 1% BSA and stained with B220-BV510 (RA3-6B2; BD), anti-GFP–Dylight 488 and anti-Syk (pY352)–Alexa Fluor 647 (17A/P-ZAP70; BD), anti-Akt (pS473)–Alexa Fluor 647 (M89-61; BD), or isotype control (MOPC-21; BD) at room temperature for 30–45 min. The cells were washed twice, and events were collected on an LSRII or Fortessa X-20 flow cytometer (BD) and analyzed using FlowJo software (Tree Star).

Analysis of calcium mobilization

For measurements of intracellular free calcium concentration ($[Ca^{2+}]_i$), splenocytes (2×10^7/ml in IMDM medium containing 2% FCS) were simultaneously stained with anti-B220–APC and loaded with 5 µM Indo-1 acetoxymethyl (Indo1-AM; Molecular Probes) for 30 min at room temperature. After washing once with IMDM with 2% FCS, the cells were resuspended at 10^7 cells/ml in warm IMDM with 2% FCS in a 500-µl volume. Indo-1 was excited with a 355-nm laser, Ca^{2+}-bound Indo-1 was detected using a 379/28 bandpass filter, and unbound Indo-1 was detected using a 524/40 bandpass filter. Relative free calcium concentration was determined by the ratio of bound/unbound Indo-1. After the baseline was established by analysis for 30 s, cells were stimulated with the indicated dose of $F(Ab')_2$ goat anti–mouse IgM (anti-µ; Jackson ImmunoResearch Laboratories, Inc.), $F(Ab')_2$ rabbit anti–mouse IgG (H+L; Invitrogen), anti-IgM (b-7-6), or anti-IgD (1-3-5) for 2 min. Relative mean $[Ca^{2+}]_i$ was measured using an LSR II or Fortessa X-20 flow cytometer with analysis using FlowJo software. To quantify the calcium response, we calculated the area under the curve. For statistical analysis of all experiments, in each experiment, the response of B cells from infected mice was normalized to the response of B cells from sham controls.

Immunoblotting

B cells from donor mice were enriched for by depletion of $CD43^+$ cells with anti-CD43–conjugated magnetic beads (magnetic-activated cell-sorting anti–mouse CD43; Miltenyi Biotec). Resultant populations were >97% B cells based on B220 staining and FACS analysis. Cells were lysed in 1% NP-40 lysis buffer (1% Nonidet P-40, 150 mM NaCl, 10 mM Tris, pH 7.5, 10 mM sodium pyrophosphate, 2 mM sodium orthovanadate, 1 mM PMSF, 10 mM NaF, 0.4 mM EDTA, 1 mM aprotinin, 1 mM α-1-antitrypsin, and 1 mM leupeptin). For analysis of CD19 phosphorylation, Tris was adjusted to 50 mM, and 0.1% SDS was added. For analysis of whole-cell lysates (WCLs), detergent lysates ($0.5–1 \times 10^6$ cell equivalents) were mixed with an equal volume of 2× reducing SDS sample buffer. For immunoprecipitation, WCLs (10×10^6 cell equivalents) were incubated with Sepharose 6B beads to preclear the WCLs of nonspecific bead-binding proteins. Precleared WCL was incubated with antibody (anti–SHIP-1, Syk, or Dok-1)-conjugated Sepharose 6B beads. The Sepharose beads were washed five times and mixed with reducing SDS sample buffer. Samples were boiled for 5 min, and proteins were separated by SDS-PAGE and transferred to polyvinylidene fluoride membranes, which were then blocked with TBS-based Odyssey block buffer (LI-COR Biosciences) or 5% milk in TBS–0.05% Tween 20. Antibodies specific for SHIP-1, Dok-1 (affinity-purified polyclonal rabbit antibodies prepared in our laboratory, generated by immunization with aa residues 909–959 of mouse SHIP and full-length mouse $p62^{dok}$, respectively), PTEN (Cell Signaling Technology), CD19 (Santa Cruz Biotechnology, Inc.), pCD19 (Tyr 531; Cell Signaling Technology), pAkt (S473; Cell Signaling Technology), pPLCγ2 (Tyr1217; Cell Signaling Technology), p44/42 MAPK (Erk1/2; Thr202/Tyr204; Cell Signaling Technology), PCLγ2 (Cell Signaling Technology), pan Erk (BD), Akt (Cell Signaling Technology), Syk (Santa Cruz Biotechnology, Inc.), pTyr (4G10), or actin (Cell Signaling Technology) were diluted in Odyssey block buffer or 3% BSA–TBS–0.05% Tween 20 (pCD19 and CD19). Antibody binding was detected using the Odyssey system (LI-COR Biosciences) in conjunction with secondary antibodies specific for native mouse (Trueblot) or rabbit (Trueblot) immunoglobulin (eBioscience) directly conjugated to one of two fluorophores (IR680 or IR800),

goat anti–rabbit IgG–Alexa Fluor 680 (Invitrogen), or goat anti–mouse IgG–Alexa Fluor 680 (LI-COR Biosciences). Alternatively, transferred proteins were visualized using HRP-labeled antibodies followed by enhanced chemiluminescence (NEN) and detection by film or the ChemiDoc XRS Imagining system (Bio-Rad Laboratories).

Migration assay

Quantitative chemotaxis assays were conducted using transwells (6.5-mm diameter, 5-µm pore size, and polycarbonate membrane; Costar). 10^6 purified B cells from γHV68-infected mice (7 d.p.i.) or sham-infected mice in 100 µl of 5% FCS IMDM were placed in each upper chamber. Recombinant mouse CXCL12/SDF-1α (R&D Systems) was added at the indicated concentrations to the lower chamber (600 µl volume), and the cells were incubated at 37°C for 3.5 h. After the incubation, the migrated (lower chamber) cells were counted. 100% migration was obtained by counting cells added directly to the lower chamber.

Hemagglutination assay

Serum was serially diluted (twofold) in HBSS in V-bottom microtiter plates in a 50-µl volume. Then, 50 µl of 0.5% SRBC suspension in HBSS was added to each well, and plates were incubated at 37°C for 1 h. The hemagglutination titer was defined as the reciprocal value of the highest serum dilution at which hemagglutination of SRBCs was detected.

ELISPOT

For detection of IgM^a anti-HEL antibodies, microtiter plates were coated with 10 µg/ml HEL in PBS overnight and blocked with 2% BSA in PBS 0.05% Tween 20. Before use, the plates were washed twice with PBS and once with complete medium (IMDM supplemented with 10% FCS, 1 mM sodium pyruvate, 2 mM L-glutamine, 100 U/ml penicillin/streptomycin, 50 mg/ml gentamicin, and 0.1 mM 2-Me.). Spleens were disrupted in complete medium, and RBCs were lysed using ammonium chloride Tris. Twofold serial dilutions were made beginning with 1/100th of a spleen in the first well. The plates were incubated at 37°C for 6 h or overnight. MD4-derived antibodies bound to HEL were detected using biotinylated DS-1 (anti-IgM^a), followed by streptavidin–alkaline phosphatase (SouthernBiotech). Between steps, plates were washed four times with PBS–0.05% Tween 20. The plates were developed by incubation with ELISPOT development buffer (25 µM 5-bromo-chloro-3-indolyl phosphate p-toluidine, 100 mM NaCl, 100 mM Tris, and 10 mM $MgCl_2$, pH 9.5) for 1 h. The reaction was stopped by washing the plate three times with double-distilled H_2O. The number of spots at a cell dilution in the linear range was determined, and the number of antibody-secreting cells (ASCs) per spleen was calculated.

Statistics

Data were analyzed using Prism (GraphPad Software). Most experiments were analyzed using a both-tailed unpaired Student's *t* test. In Figs. 1 (A and F), 2 C, and 3 H, normalized data from several independent experiments were analyzed. Normalization was done by dividing the value of the infected group by the value of the sham-infected group. Mean values of individual experiments were used in Fig. 1 F and Fig. 3 H. As a result, the control group always has the value 1. The data were transformed to a log2 scale and were tested for the hypothesis that the mean of the log-transformed data from infected individuals differ from zero using a both-tailed one-sample Student's *t* test followed by a Bonferroni adjustment. P-values >0.05 were not considered statistically significant. ns, $P > 0.05$; *, $P < 0.05$; **, $P < 0.01$; ***, $P < 0.001$.

ACKNOWLEDGMENTS

We thank Drs. M. Shlomchik, R. Rickert, and K. Rajewsky for mice and Dr. K. Hasenkrug for the LDV stock. We thank Dr. Jennifer Matsuda and her outstanding staff at the National Jewish Health Mouse Genetics Facility for construction of the Rosa26-STOPflox-*PTEN*-2A-YFP mouse.

This study was supported by the following National Institutes of Health grants: RO1 AI077597, RO1 DK096492, RO1 AI124487, PO1 AI22295 (J.C. Cambier), and R01 GM117946 (P. Rudra).

The authors declare no competing financial interests.

Author contributions: A. Getahun and S.M. Wemlinger performed the experiments. M.L. Santiago and L.F. van Dyk provided essential reagents and intellectual input. P. Rudra did the statistical analysis. A. Getahun and J.C. Cambier designed the experiments, analyzed the data, and wrote the paper.

Submitted: 24 June 2016
Revised: 23 October 2016
Accepted: 30 January 2017

REFERENCES

Akerlund, J., A. Getahun, and J.C. Cambier. 2015. B cell expression of the SH2-containing inositol 5-phosphatase (SHIP-1) is required to establish anergy to high affinity, proteinacious autoantigens. *J. Autoimmun.* 62:45–54. http://dx.doi.org/10.1016/j.jaut.2015.06.007

Anzelon, A.N., H. Wu, and R.C. Rickert. 2003. Pten inactivation alters peripheral B lymphocyte fate and reconstitutes CD19 function. *Nat. Immunol.* 4:287–294. http://dx.doi.org/10.1038/ni892

Avota, E., H. Harms, and S. Schneider-Schaulies. 2006. Measles virus induces expression of SIP110, a constitutively membrane clustered lipid phosphatase, which inhibits T cell proliferation. *Cell. Microbiol.* 8:1826–1839. http://dx.doi.org/10.1111/j.1462-5822.2006.00752.x

Barton, E.S., D.W. White, J.S. Cathelyn, K.A. Brett-McClellan, M. Engle, M.S. Diamond, V.L. Miller, and H.W. Virgin IV. 2007. Herpesvirus latency confers symbiotic protection from bacterial infection. *Nature.* 447:326–329. http://dx.doi.org/10.1038/nature05762

Benedict, C.A., C. De Trez, K. Schneider, S. Ha, G. Patterson, and C.F. Ware. 2006. Specific remodeling of splenic architecture by cytomegalovirus. *PLoS Pathog.* 2:e16. http://dx.doi.org/10.1371/journal.ppat.0020016

Brauweiler, A., K. Merrell, S.B. Gauld, and J.C. Cambier. 2007. Cutting Edge: Acute and chronic exposure of immature B cells to antigen leads to impaired homing and SHIP1-dependent reduction in stromal cell-derived factor-1 responsiveness. *J. Immunol.* 178:3353–3357. http://dx.doi.org/10.4049/jimmunol.178.6.3353

Brown, M.G., A.O. Dokun, J.W. Heusel, H.R.C. Smith, D.L. Beckman, E.A. Blattenberger, C.E. Dubbelde, L.R. Stone, A.A. Scalzo, and W.M. Yokoyama. 2001. Vital involvement of a natural killer cell activation

receptor in resistance to viral infection. *Science.* 292:934–937. http://dx.doi.org/10.1126/science.1060042

Browne, C.D., C.J. Del Nagro, M.H. Cato, H.S. Dengler, and R.C. Rickert. 2009. Suppression of phosphatidylinositol 3,4,5-trisphosphate production is a key determinant of B cell anergy. *Immunity.* 31:749–760. http://dx.doi.org/10.1016/j.immuni.2009.08.026

Ceglowski, W.S., B.P. Campbell, and H. Friedman. 1975. Immunosuppression by leukemia viruses. Effect of Friend leukemia virus on humoral immune competence of leukemia-resistant C57BL/6 mice. *J. Immunol.* 114:231–236.

Cooke, M.P., A.W. Heath, K.M. Shokat, Y. Zeng, F.D. Finkelman, P.S. Linsley, M. Howard, and C.C. Goodnow. 1994. Immunoglobulin signal transduction guides the specificity of B cell-T cell interactions and is blocked in tolerant self-reactive B cells. *J. Exp. Med.* 179:425–438. http://dx.doi.org/10.1084/jem.179.2.425

Elsner, R.A., C.J. Hastey, K.J. Olsen, and N. Baumgarth. 2015. Suppression of long-lived humoral immunity following *Borrelia burgdorferi* infection. *PLoS Pathog.* 11:e1004976. http://dx.doi.org/10.1371/journal.ppat.1004976

Furman, D., V. Jojic, S. Sharma, S.S. Shen-Orr, C.J.L. Angel, S. Onengut-Gumuscu, B.A. Kidd, H.T. Maecker, P. Concannon, C.L. Dekker, et al. 2015. Cytomegalovirus infection enhances the immune response to influenza. *Sci. Transl. Med.* 7:281ra43. http://dx.doi.org/10.1126/scitranslmed.aaa2293

Getahun, A., M.J. Smith, I. Kogut, L.F. van Dyk, and J.C. Cambier. 2012. Retention of anergy and inhibition of antibody responses during acute γ herpesvirus 68 infection. *J. Immunol.* 189:2965–2974. http://dx.doi.org/10.4049/jimmunol.1201407

Getahun, A., N.A. Beavers, S.R. Larson, M.J. Shlomchik, and J.C. Cambier. 2016. Continuous inhibitory signaling by both SHP-1 and SHIP-1 pathways is required to maintain unresponsiveness of anergic B cells. *J. Exp. Med.* 213:751–769. http://dx.doi.org/10.1084/jem.20150537

Goodnow, C.C., J. Crosbie, S. Adelstein, T.B. Lavoie, S.J. Smith-Gill, R.A. Brink, H. Pritchard-Briscoe, J.S. Wotherspoon, R.H. Loblay, K. Raphael, et al. 1988. Altered immunoglobulin expression and functional silencing of self-reactive B lymphocytes in transgenic mice. *Nature.* 334:676–682. http://dx.doi.org/10.1038/334676a0

Holder, B., D.J. Miles, S. Kaye, S. Crozier, N.I. Mohammed, N.O. Duah, E. Roberts, O. Ojuola, M.S. Palmero, E.S. Touray, et al. 2010. Epstein-Barr virus but not cytomegalovirus is associated with reduced vaccine antibody responses in Gambian infants. *PLoS One.* 5:e14013. http://dx.doi.org/10.1371/journal.pone.0014013

Howard, R.J., and J.S. Najarian. 1974. Cytomegalovirus-induced immune suppression. I. Humoral immunity. *Clin. Exp. Immunol.* 18:109–118.

Isakov, N., M. Feldman, and S. Segal. 1982. The mechanism of modulation of humoral immune responses after infection of mice with lactic dehydrogenase virus. *J. Immunol.* 128:969–975.

Khalil, A.M., J.C. Cambier, and M.J. Shlomchik. 2012. B cell receptor signal transduction in the GC is short-circuited by high phosphatase activity. *Science.* 336:1178–1181. http://dx.doi.org/10.1126/science.1213368

Kirchenbaum, G.A., J.B. St Clair, T. Detanico, K. Aviszus, and L.J. Wysocki. 2014. Functionally responsive self-reactive B cells of low affinity express reduced levels of surface IgM. *Eur. J. Immunol.* 44:970–982. http://dx.doi.org/10.1002/eji.201344276

Li, S., M. Zhu, R. Pan, T. Fang, Y.-Y. Cao, S. Chen, X. Zhao, C.-Q. Lei, L. Guo, Y. Chen, et al. 2016. The tumor suppressor PTEN has a critical role in antiviral innate immunity. *Nat. Immunol.* 17:241–249. http://dx.doi.org/10.1038/ni.3311

Marques, R., I. Antunes, U. Eksmond, J. Stoye, K. Hasenkrug, and G. Kassiotis. 2008. B lymphocyte activation by coinfection prevents immune control of friend virus infection. *J. Immunol.* 181:3432–3440. http://dx.doi.org/10.4049/jimmunol.181.5.3432

Martin, A.P., C. Canasto-Chibuque, L. Shang, B.J. Rollins, and S.A. Lira. 2006. The chemokine decoy receptor M3 blocks CC chemokine ligand 2 and CXC chemokine ligand 13 function in vivo. *J. Immunol.* 177:7296–7302. http://dx.doi.org/10.4049/jimmunol.177.10.7296

Matar, C.G., N.R. Anthony, B.M. O'Flaherty, N.T. Jacobs, L. Priyamvada, C.R. Engwerda, S.H. Speck, and T.J. Lamb. 2015. Gammaherpesvirus co-infection with malaria suppresses anti-parasitic humoral immunity. *PLoS Pathog.* 11:e1004858. http://dx.doi.org/10.1371/journal.ppat.1004858

Michaelides, M.C., and E.S. Simms. 1977. Immune responses in mice infected with lactic dehydrogenase virus. I. Antibody response to DNP-BGG and hyperglobulinaemia in BALB/c mice. *Immunology.* 32:981–988.

Mueller, S.N., K.A. Hosiawa-Meagher, B.T. Konieczny, B.M. Sullivan, M.F. Bachmann, R.M. Locksley, R. Ahmed, and M. Matloubian. 2007. Regulation of homeostatic chemokine expression and cell trafficking during immune responses. *Science.* 317:670–674. http://dx.doi.org/10.1126/science.1144830

Notkins, A.L., S.E. Mergenhagen, and R.J. Howard. 1970. Effect of virus infections on the function of the immune system. *Annu. Rev. Microbiol.* 24:525–538. http://dx.doi.org/10.1146/annurev.mi.24.100170.002521

Robertson, S.J., C.G. Ammann, R.J. Messer, A.B. Carmody, L. Myers, U. Dittmer, S. Nair, N. Gerlach, L.H. Evans, W.A. Cafruny, and K.J. Hasenkrug. 2008. Suppression of acute anti-friend virus $CD8^+$ T-cell responses by coinfection with lactate dehydrogenase-elevating virus. *J. Virol.* 82:408–418. http://dx.doi.org/10.1128/JVI.01413-07

Santiago, M.L., M. Montano, R. Benitez, R.J. Messer, W. Yonemoto, B. Chesebro, K.J. Hasenkrug, and W.C. Greene. 2008. *Apobec3* encodes *Rfv3*, a gene influencing neutralizing antibody control of retrovirus infection. *Science.* 321:1343–1346. http://dx.doi.org/10.1126/science.1161121

Song, M.S., L. Salmena, and P.P. Pandolfi. 2012. The functions and regulation of the PTEN tumour suppressor. *Nat. Rev. Mol. Cell Biol.* 13:283–296.

Srinivas, S., T. Watanabe, C.S. Lin, C.M. William, Y. Tanabe, T.M. Jessell, and F. Costantini. 2001. Cre reporter strains produced by targeted insertion of EYFP and ECFP into the ROSA26 locus. *BMC Dev. Biol.* 1:4. http://dx.doi.org/10.1186/1471-213X-1-4

Srinivasan, L., Y. Sasaki, D.P. Calado, B. Zhang, J.H. Paik, R.A. DePinho, J.L. Kutok, J.F. Kearney, K.L. Otipoby, and K. Rajewsky. 2009. PI3 kinase signals BCR-dependent mature B cell survival. *Cell.* 139:573–586. http://dx.doi.org/10.1016/j.cell.2009.08.041

Stevenson, P.G., and P.C. Doherty. 1998. Kinetic analysis of the specific host response to a murine gammaherpesvirus. *J. Virol.* 72:943–949.

Virgin, H.W. IV, P. Latreille, P. Wamsley, K. Hallsworth, K.E. Weck, A.J. Dal Canto, and S.H. Speck. 1997. Complete sequence and genomic analysis of murine gammaherpesvirus 68. *J. Virol.* 71:5894–5904.